RL-TR-92-231
In-House Report
August 1992



# THE EFFECTS OF FINITE SCATTERING AREA ON THE BISTATIC NORMALIZED CROSS SECTION FOR A TWO DIMENSIONAL ROUGH SURFACE

Lisa M. Mockapetris



*APPROVED FOR PUBLIC RELEASE; DISTRIBUTION UNLIMITED.*



Rome Laboratory
Air Force Materiel Command
Griffiss Air Force Base, New York

This report has been reviewed by the Rome Laboratory Public Affairs Office (PA) and is releasable to the National Technical Information Service (NTIS). At NTIS it will be releasable to the general public, including foreign nations.

RL-TR-92-231 has been reviewed and is approved for publication.

APPROVED: Edward E. Altshuler

EDWARD E. ALTSHULER
Chief, Applied Electromagnetics Division
Electromagnetics & Reliability Directorate

FOR THE COMMANDER: John K. Schindler

JOHN K. SCHINDLER, Director
Electromagnetics & Reliability Directorate

If your address has changed or if you wish to be removed from the Rome Laboratory mailing list, or if the addressee is no longer employed by your organization, please notify RL(ERCE ) Hanscom AFB MA 01731-5000. This will assist us in maintaining a current mailing list.

Do not return copies of this report unless contractual obligations or notices on a specific document require that it be returned.

# REPORT DOCUMENTATION PAGE

*Form Approved*
*OMB No. 0704-0188*



| 1. AGENCY USE ONLY *(Leave blank)* | 2. REPORT DATE | 3. REPORT TYPE AND DATES COVERED |
|---|---|---|
| | August 1992 | In-House 23 July 1992 |

**4. TITLE AND SUBTITLE**

The Effects of Finite Scattering Area on the Bistatic Normalized Cross Section for a Two-Dimensional Rough Surface

**5. FUNDING NUMBERS**

PE: 61102F
PR: 2305
TA: 2305J4
WU: 2305J409

**6. AUTHOR(S)**

Lisa M. Mockapetris

**7. PERFORMING ORGANIZATION NAME(S) AND ADDRESS(ES)**

Rome Labratory/ERCE
Hanscom AFB MA 01731-5000

**8. PERFORMING ORGANIZATION REPORT NUMBER**

RL-TR-92-231

**9. SPONSORING/MONITORING AGENCY NAME(S) AND ADDRESS(ES)**

**10. SPONSORING/MONITORING AGENCY REPORT NUMBER**

**11. SUPPLEMENTARY NOTES**

**12a. DISTRIBUTION/AVAILABILITY STATEMENT**

Approved for public release; distribution unlimited

**12b. DISTRIBUTION CODE**

**13. ABSTRACT** *(Maximum 200 words)*

In this report, cell size effects on the bistatic normalized scattering cross section are studied for two-dimensional rough surfaces as a function of signal wavelength and surface parameters. In previous studies the finite cell size effects were analyzed for one-dimensional surfaces. The introduction of the two-dimensional roughness produces additional features since the bistatic scattering now extends to out-of-plane angles. This allows the signal to undergo depolarization as it is scattered from the surface. Copolarized and cross polarized scattering cross section patterns are presented as a function of azimuthal angle for various cell sizes. The depolarization introduces complicated minima structure in the copolarized results. Two limiting case comparisons are examined. As the azimuthal extent of the cell is decreased, the limiting results approach those for the one-dimensional rough surface. Finally, as the cell size is increased, the two-dimensional scattering patterns take on the form of the infinite scattering cell solution for a two-dimensional rough surface.

**14. SUBJECT TERMS**

Finite cell scattering
Two dimensional roughness
Bistatic scattering
Polarization
Rough surface scattering

**15. NUMBER OF PAGES**

34

**16. PRICE CODE**

| 17. SECURITY CLASSIFICATION OF REPORT | 18. SECURITY CLASSIFICATION OF THIS PAGE | 19. SECURITY CLASSIFICATION OF ABSTRACT | 20. LIMITATION OF ABSTRACT |
|---|---|---|---|
| UNCLASSIFIED | UNCLASSIFIED | UNCLASSIFIED | SAR |

NSN 7540-01-280-5500

Standard Form 298 (Rev. 2-89)
Prescribed by ANSI Std. 239-18
298-102

# Contents

## Illustrations

## Illustrations

# The Effects Of Finite Scattering Area On The Bistatic Normalized Cross Section For A Two-Dimensional Rough Surface

## 1. INTRODUCTION

High-range-resolution radars illuminate a small patch of ground in the range dimension. This smaller clutter patch can reduce the total radar clutter and therefore make target detection easier, so long as the characteristics of the clutter are unchanged. However, many of the assumptions of how clutter will behave in a radar system assume the clutter cell is infinite compared to the separation of the scattering elements. When the dimensions of the cell shrink to just a few correlation lengths of the roughness, the characteristics of the clutter are no longer well known.

Previous reports by Papa and Woodworth[1] and by Sharpe[2,3] have considered finite cell size scattering from a one-dimensionally rough surface. These reports suggest that the cell size can have a significant effect on the scattering statistics. In this report, the normalized clutter cross section of two-dimensionally rough surfaces is examined for finite cell sizes. The two-dimensional case is more involved than one-dimensional scattering because off-axis scattering and depolarization of the scattered wave must be taken into account.

In this report, the calculated mean values of the co-polarized and cross polarized normalized cross section $\sigma^0$, for finite cell sizes, are determined as a function of scattering configuration. The effect of varying the cross range dimension of the clutter cell, the wavelength of the incident field, and the rms height of the rough surface are also studied. The results are then compared to $\sigma^0$ values for the one-dimensional finite cell model and for the infinite cell size scattering analyses. Since surface dielectric constant $\varepsilon_r$ does not affect the finite cell size effects, the results are given for a perfectly conducting surface. The effect of $\varepsilon_r$ is just multiplicative. However, $\varepsilon_r$ will affect the angular dependence of the mean normalized cross section.

(Received for publication 28 August 1992)

## 2. THEORETICAL DEVELOPMENT

The normalized cross section of a rough surface is given by:

$$\sigma^o = \lim_{R\to\infty} \frac{4\pi R_o^2}{A_c}\left(\left\langle\left|\frac{E_s}{E_i}\right|^2\right\rangle - \left\langle\left|\frac{E_s}{E_i}\right|\right\rangle^2\right) \tag{1}$$

$E_i$ is the field incident upon the rough surface and $E_S$ is the scattered field. Because $E_S$ is the field scattered by a random surface, it must be described statistically. The symbol <·> denotes an ensemble average over the variables $\zeta_1$ and $\zeta_2$, which are the random surface heights at two points, $x_1$ and $x_2$ on the surface, and $\mu_1$ and $\mu_2$, which are the surface slopes at these points. A = $L_x L_y$ is the area of the clutter cell where $L_x$ is the range dimension and $L_y$ is the azimuth dimension. $R_O$ is the distance from the surface to the point at which $E_S$ is measured. This distance must be large. The surface geometry is shown in Figure 1.

The scattered field, $E_S$, is found by solving the Helmholtz integral equation in the far field:

$$E_s = \frac{1}{4\pi}\iint_s \left(E\frac{\partial\Psi}{\partial n} - \Psi\frac{\partial E}{\partial n}\right)dxdy \tag{2}$$

where $\Psi = \dfrac{e^{ikR_o - i\vec{k}_s\cdot\vec{r}}}{R}$ is the spherical Green's function with $\vec{k}_s$ being the wave vector of the scattered field. $E$ is once again the total field on the surface given by $E = (1+R)E_i$ where $R$ is the Fresnel reflection coefficient of the surface. The normal to the surface, n, is given by:

$$\vec{n} = \frac{-\zeta_x'\hat{x} - \zeta_y'\hat{y} + \hat{z}}{\sqrt{1+\zeta_x^2+\zeta_y^2}} \tag{3}$$

Figure 2 illustrates the scattering geometry with the various parameters defined. For the perfectly conducting surface used here $R = \pm 1$ and one obtains the expression for the scattered field as:

$$E_s = \frac{-ike^{ikR_o}}{4\pi R_o} F\iint_s e^{i\vec{v}\cdot\vec{r}}dxdy \tag{4}$$

$$F = 2R\frac{(1+\cos\theta_i\cos\theta_s - \sin\theta_i\sin\theta_s\cos\phi_s)}{\cos\theta_i + \cos\theta_s}$$

where:

$$\vec{v} = k\left[(\sin\theta_i - \sin\theta_s\cos\phi_s)\hat{x} - \sin\theta_s\sin\phi_s\hat{y} - (\cos\theta_i + \cos\theta_s)\hat{z}\right]$$

$$\vec{r} = x\hat{x}_o + y\hat{y}_o + \zeta(x,y)\hat{z}_o$$

The incident field is a plane wave given by:

$$E_i = e^{ikR} \tag{5}$$

The ratio of the scattered field to the incident field is then given by:

$$\frac{E_s}{E_i} = \frac{-ikF}{4\pi R_o} \int_{-L_x/2}^{L_x/2} \int_{-L_y/2}^{L_y/2} e^{i\vec{w}\cdot\vec{r}}\, dx\, dy = \frac{-ikF}{4\pi R_o} \int_{-L_x/2}^{L_x/2} \int_{-L_y/2}^{L_y/2} e^{i(v_x x + v_y y + \zeta v_z)}\, dx\, dy \tag{6}$$

The expression for $\sigma^0$ can then be written as:

$$\sigma^o = \frac{k^2F^2}{4\pi A} \iiint \int_{-L/2}^{L/2} e^{i(v_x\tau_x + v_y\tau_y)} \left[\chi_2 - \chi_1\chi_1^*\right] dx_1 dx_2 dy_1 dy_2 \tag{7}$$

where:

$$\tau_x = |x_1 - x_2|$$

$$\tau_y = |y_1 - y_2|$$

$$\chi_1 = \left\langle e^{iv_z\zeta} \right\rangle = e^{-\Sigma'}$$

$\Sigma = \sigma v_Z$ = Rayleigh roughness parameter

$$\chi_2 = \left\langle e^{iv_z(\zeta_1 - \zeta_2)} \right\rangle = exp\left(-v_z^2\sigma^2(1 - C)\right)$$

$$C = e^{-\tau'/T'}$$

$$\tau = \sqrt{\tau_x^2 + \tau_y^2}$$

This fourfold integral can be further simplified by using a change of variables technique[3] that results in the simplified expression for $\sigma^o$:

$$\sigma^o = \frac{k^2F^2}{\pi A} \int_0^L \int \cos(v_x\tau_x)\cos(v_y\tau_y)\left[\chi_2 - \chi_1\chi_1^*\right]\left[L_x - \tau_x\right]\left[L_y - \tau_y\right] d\tau_x d\tau_y \tag{8}$$

This allows us to calculate the mean clutter cross section for rectangular cell sizes of different dimensions given by $L_x$ and $L_y$. The equation for the variance of the of the clutter cross section for a two dimensionally rough surface is given as an eight-fold integral. Because of the numerical complexity required to solve these equations, the two dimensional variance is not included in this study.

For a two dimensionally rough surface, off-axis scattering will occur and will result in depolarization of the linear polarization state of the incident wave upon reflection from the surface. The value of the clutter cross section given in Eq.(8) is for the polarization which results in the maximum value of the clutter cross section. In order to determine the horizontally and

vertically polarized components of the clutter cross section, the polarization term $F$ used in Eq.(8) must be removed and the pure scattering matrix elements given in Eqs.(10) are used. The symbol $\sigma^o_{unpol}$ will be used to represent the clutter cross section with no polarization dependence. The polarization dependent terms can then be written as:

$$\sigma^o_{pq} = \left|R_{pq}\right|^2 \sigma^o_{unpol} \tag{9}$$

The subscripts p and q refer to the polarization of the scattered wave and the incident wave respectively. For vertical and horizontal polarization states, the scattering matrix elements are given by:

$$R_{hh} = \frac{\sin\theta_i \sin\theta_s \sin^2\phi_s R_{\parallel}(\iota) + a_2 a_3 R_{\perp}(\iota)}{4\sin^2\iota \cos^2\iota} \tag{10a}$$

$$R_{vh} = -\sin\phi_s \frac{\sin\theta_s a_2 R_{\parallel}(\iota) - \sin\theta_i a_3 R_{\perp}(\iota)}{4\sin^2\iota \cos^2\iota} \tag{10b}$$

$$R_{hv} = -\sin\phi_s \frac{-\sin\theta_i a_3 R_{\parallel}(\iota) + \sin\theta_s a_2 R_{\perp}(\iota)}{4\sin^2\iota \cos^2\iota} \tag{10c}$$

$$R_{vv} = \frac{a_3 \sin\theta_i R_{\parallel}(\iota) - \sin\theta_i \sin\theta_s \sin^2\phi_s R_{\perp}(\iota)}{4\sin^2\iota \cos^2\iota} \tag{10d}$$

where:

$$a_1 = 1 + \sin\theta_i \sin\theta_s \cos\phi_s - \cos\theta_i \cos\theta_s$$

$$a_2 = \cos\theta_i \sin\theta_s + \sin\theta_i \cos\theta_s \cos\phi_s$$

$$a_3 = \sin\theta_i \cos\theta_s + \cos\theta_i \sin\theta_s \cos\phi_s$$

$$a_4 = \cos\theta_i + \cos\theta_s$$

For the perfectly conducting surfaces used in this section of the paper, $R_{\perp} = -1$ and $R_{\parallel} = 1$. This will cause the values of the co-polarized components, $|R_{vv}|^2$ and $|R_{hh}|^2$ to be identical. Similarly, the cross polarized components, $|R_{hv}|^2$ and $|R_{vh}|^2$ are also identical. These scattering matrix elements allow us to separate the total scattered power into the co-polarized and cross polarized components.

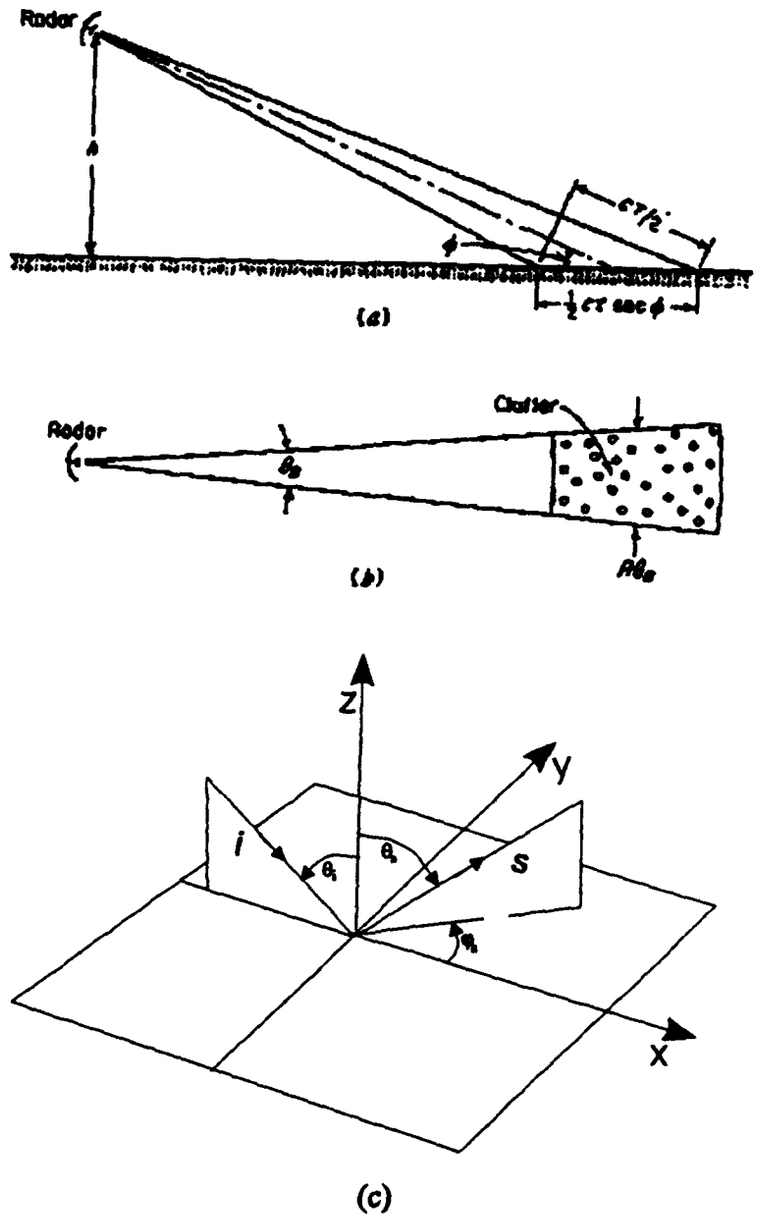


Figure 1. Resolution Cell and Scattering Angle Definitions

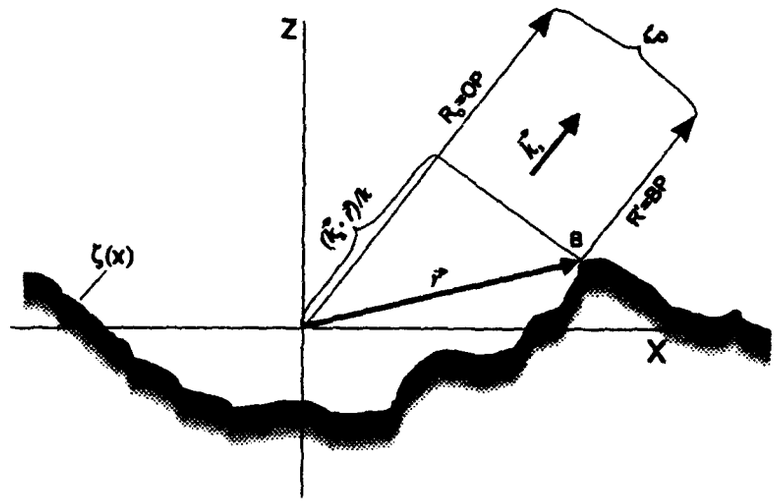


Figure 2. Scattering Geometry

## 3. RESULTS

The first major thrust shown in the results is the effect of cell size on the mean normalized cross section of surfaces which are rough in two dimensions. The area of the clutter cell is $A = L_x L_y$ where $L_x$ is the range dimension of the cell, which is determined by the pulse width, and $L_y$ is the azimuth dimension, which is a functior of antenna beamwidth.

The first set of figures examines trends in roughness and wavelength effects using surface plots of the co-polarized and cross polarized components of $\sigma^o$. The dominant feature in the patterns is the variation in the $\sigma^o$ values that result in local minima.

Figures 3 and 4 are for $\theta_i = 75^\circ$, T = 1 m, $\sigma$ = 0.2 m, $L_x$ = 2 m and $L_y$ = 2 m for a wavelength of $\lambda$ = 0.1 m. For the co-polarized component shown in Figure 3 there is a continual shift in the location of the polarization minima towards zero elevation scattering angle as the azimuth angle increases. This agrees with previously published results for scattering from infinite clutter cells[4]. In comparing the co-polarized component with the cross polarized component in Figure 4, it is clear that at the angles where there are minima in the co-polarized component, most of the energy is converted to the cross polarization. Figures 5 and 6 are surface plots of the co-polarized and cross polarized components of $\sigma^o$ for the same conditions with wavelength $\lambda$ = 0.25 m: $\theta_i = 75^\circ$, T = 1 m, $\sigma$ = 0.2 m, $L_x$ = 2 m and $L_y$ = 2 m. The large $\lambda$ implies that the surface appears relatively smoother. Figures 7 and 8 have identical parameters to Figures 5 and 6 except that $\sigma$ = 0.5m. This produces a Rayleigh roughness parameter similar to the one in Figures 3 and 4. The same trends are seen in all these cases. Differences in relative magnitudes are due to the wavelength dependence of the kernel of $\sigma^o$.

The null locations of the co-polarized component of $\sigma^o$ are, in general, functions of the scattering geometry and the dielectric constant. Because of this, these locations should not change for a finite cell size. To determine the location of the nulls more closely, Figures 9 through 11 are line plots of the co-polarized component of $\sigma^o$ for the same parameters given above. The correlation length used in these calculations was T = 1 m. The mean surface slope, defined as $\sigma$/T, is then 0.2 for Figures 9 and 10 and 0.5 for Figure 11. In both Figures 9 and 10 no null occurs for $\phi_S = 0^\circ$ and $\phi_S = 15^\circ$. For $\phi_S = 30^\circ$, the null is at $\theta_S = 70^\circ$, for $\phi_S = 45^\circ$ the null is at $\theta_S = 60^\circ$, $\phi_S = 60^\circ$ has the null at $\theta_S = 40^\circ$ and for $\phi_S = 75^\circ$ the null is at $\theta_S = 20^\circ$.

Papa, Lennon, and Taylor[4] have published bistatic scattering results for an infinite cell having the same parameters used here. The corresponding expression for $\sigma^o$ for the infinite cell size is:

$$\sigma^o = \frac{8\pi^2}{\lambda^2}\int_0^\infty J_o(v_x\tau)\left[\chi_2 - \chi_1\chi_1^*\right]\tau d\tau$$

The null locations for the finite cell size agree quite closely with the null locations given for the infinite cell size. For Figure 11 where $\sigma$/T = 0.5, very close agreement with published results of null locations is once again seen. This comparison between scattering from finite clutter cells show that for the small dimensions used in the analysis, the size of the clutter cell does not affect the location of the polarization nulls.

In order to compare values of $\sigma^o$ obtained with the two dimensional finite cell size model to the physical optics model used for the infinite cell size, the size of the finite cell was increased to 6 m x 6 m and 10 m x 10 m. These results are plotted in Figures 12 and 13. In Figure 14 the infinite cell size scattering is plotted using physical optics calculations. The trends of the cross section are very similar for the infinite cell size model and the finite cell size model. The null locations do not change at all for the two models. The discrepancy in the values of $\sigma^o$ are most significant for small values of azimuth angle and the differences become more pronounced as the scattering angle increases.

The next area of consideration is comparison with one dimensional results. Note that depolarization and off axis scattering do not occur in the one-dimensional case so differences should occur in the results for the two different cases. For the one- dimensional studies done previously, $L_y$ was zero. Figure 15 is a plot of the ratio of $\sigma^o$ for the two dimensional roughness for small $L_y$ to $\sigma^o$ for the one-dimensional case. Fairly good agreement is seen for the two models, particularly for moderate scattering angles. For extreme back scatter and extreme forward scatter, however, the two-dimensional case shows larger returns. This is due to the very small number of scattering facets in the one dimensional model that are tilted severely enough to cause scattering at these extreme angles. Because these results are for $\lambda = 0.25$ m, which is a relatively long wavelength, the surface appears fairly smooth. As the surface roughness increases, the number of properly oriented facets will increase. In the two-dimensional model, however, there are also off-axis facets that are tilted properly to contribute to the scattering in the extreme forward and back scatter directions.

For an actual high resolution radar, $L_x$ will be very small. However, $L_y$ , which is determined by the antenna beam width, may not be small. To determine the effect of $L_y$ on the clutter cross section, small values of $L_x$ were used while $L_y$ was increased. As $L_y$ increases, $\sigma^o$ does not show any significant changes. Figure 16 plots $\sigma^o$ for in-plane scattering as $L_y$ increases from one meter to 10 meters. The largest variation in clutter cross section is just a few tenths of a dB. From these two figures it is clear that the one-dimensional and the two-dimensional model agree quite closely except at extreme angles and also that the cross range dimension of the clutter cell does not have a significant effect on the value of the clutter cross section.

Figures 17 and 18 are plots of the out of plane scattering for $\theta_i = 75^o$, $\lambda = 0.25$ m, and $\sigma = 0.5$ m with $L_y = 6$ m and $L_y = 10$ m, respectively. Comparing them with Figure 11 where $L_y = 2$ m, we see that even for off axis scattering, $L_y$ has very little effect on $\sigma^o$ . The only noticeable difference is seen at large values of $\theta_s$, and even this difference is quite small.

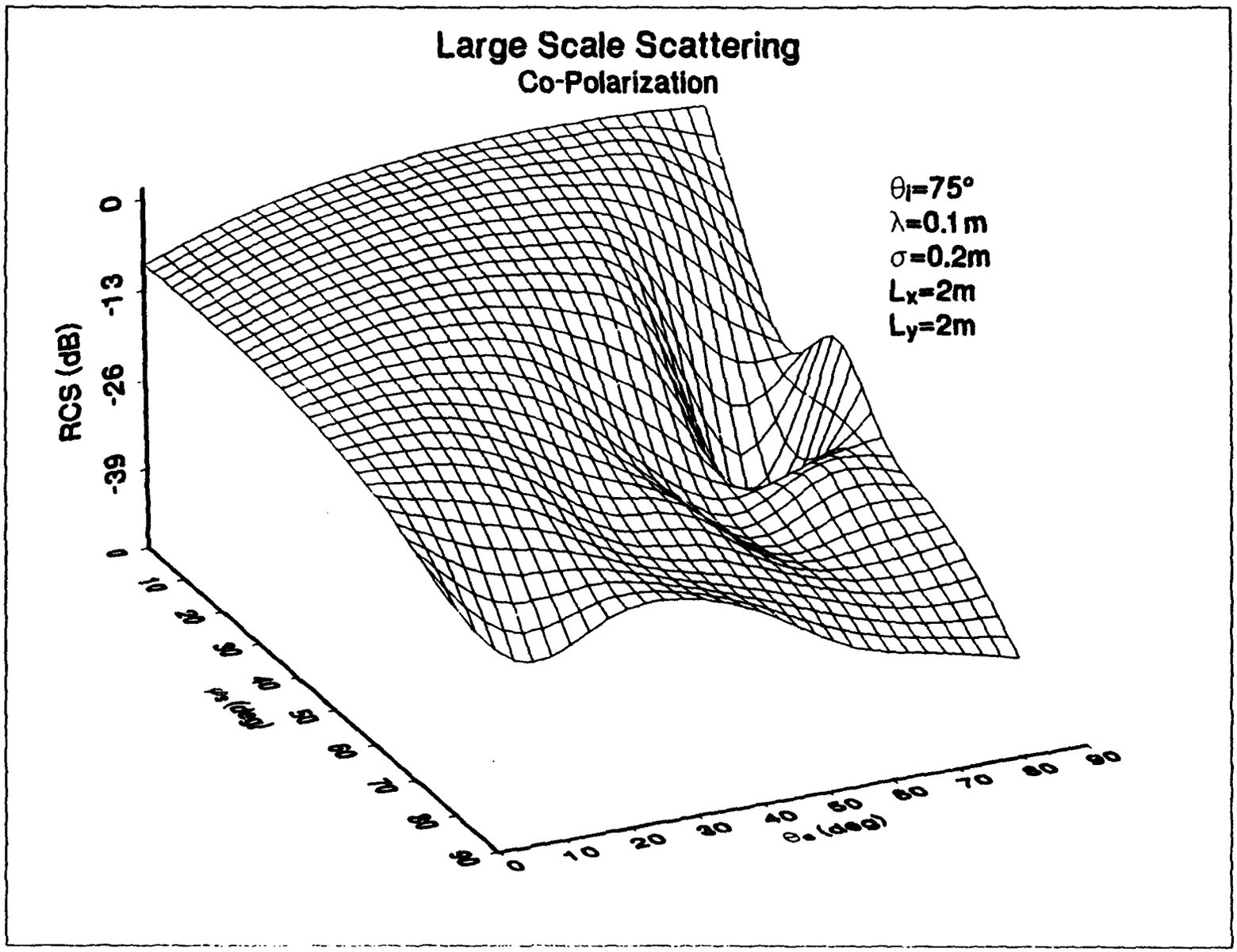


Figure 3. Co-Polarized Normalized Scattering Cross Section as a Function of Elevation and Azimuthal Angle, $\lambda = 0.1$ m and $\sigma = 0.2$ m

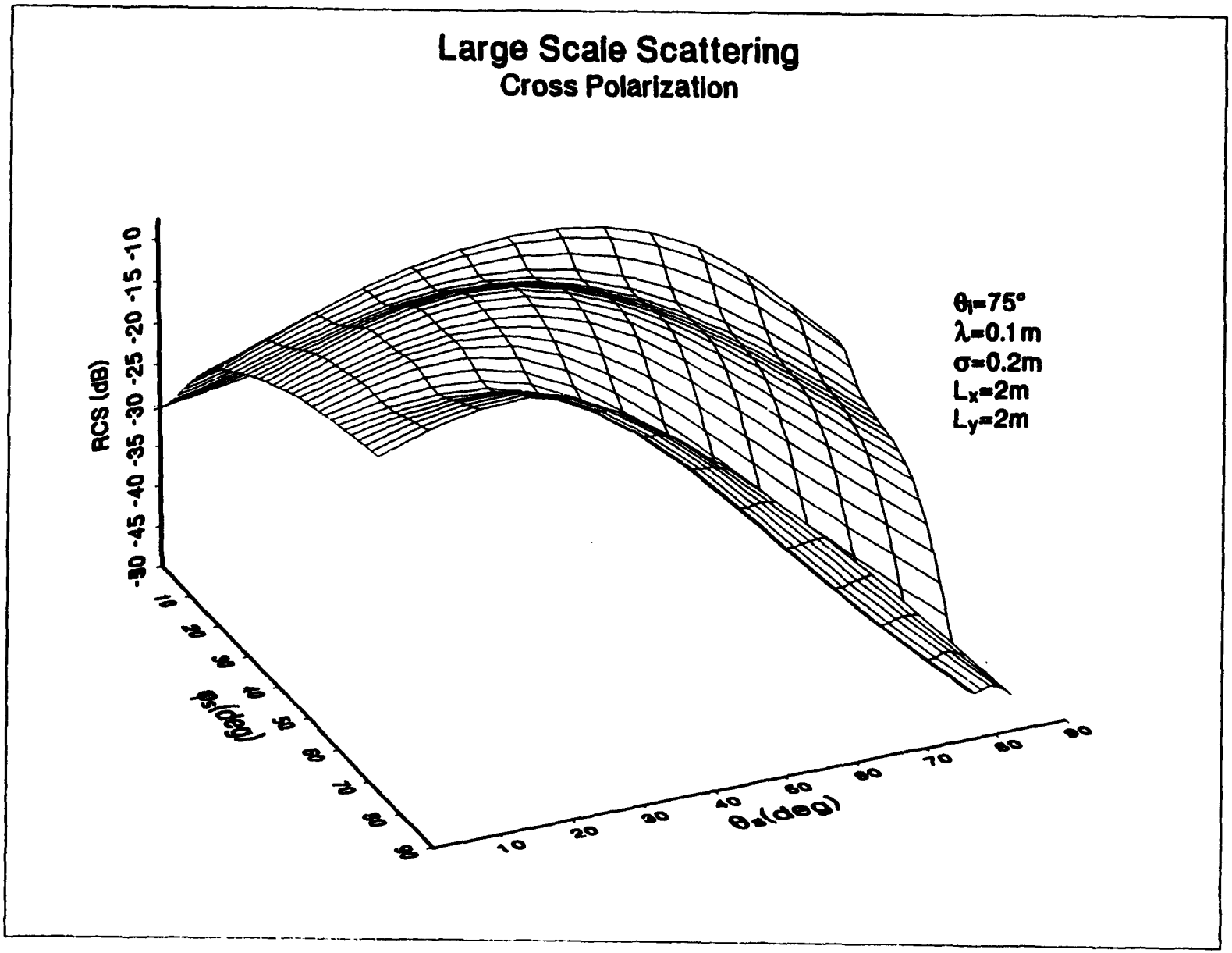


Figure 4. Cross-Polarized Normalized Scattering Cross Section as a Function of Elevation and Azimuthal Angle, $\lambda = 0.1$ m and $\sigma = 0.2$ m

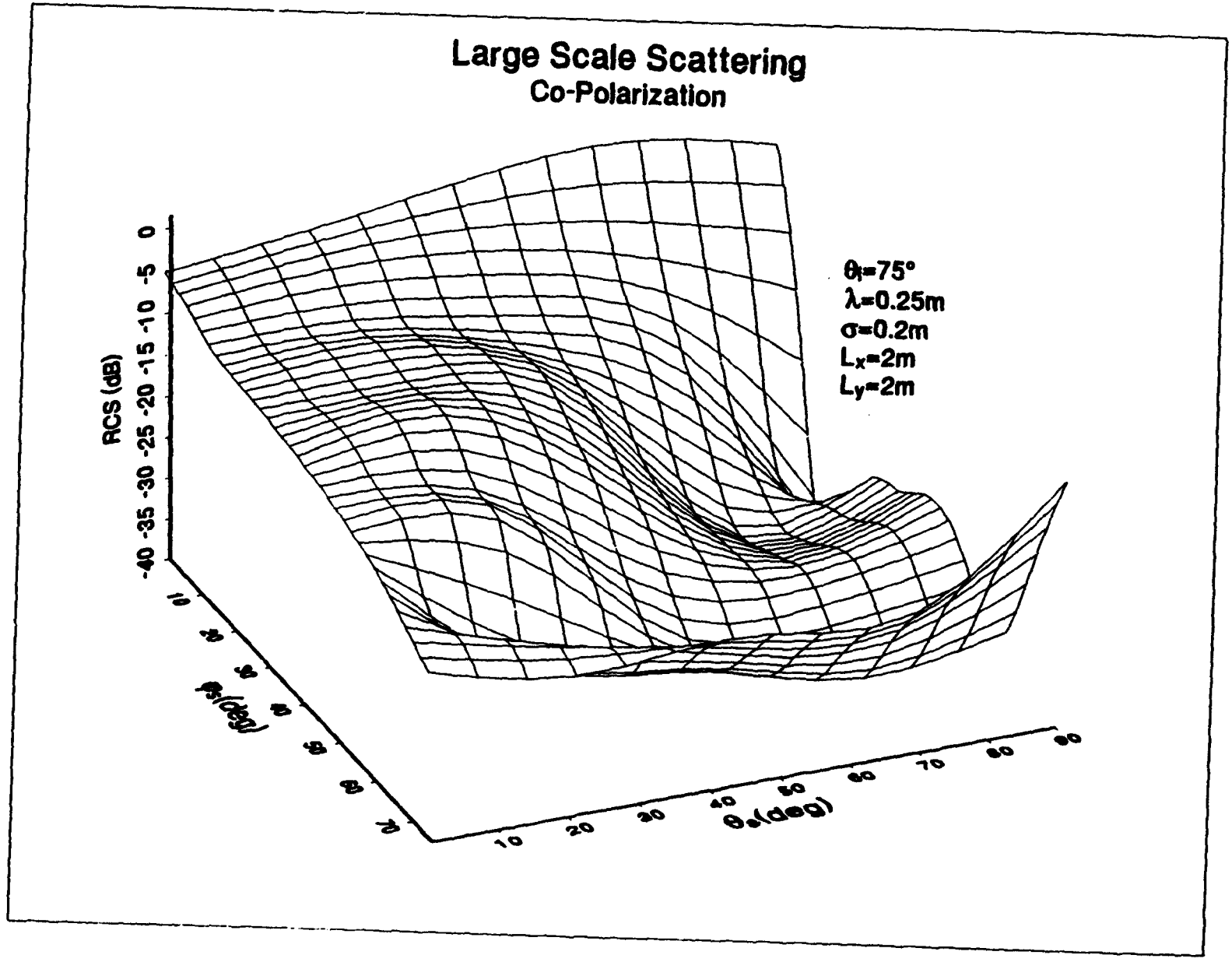


Figure 5. Co-Polarized Normalized Scattering Cross Section as a Function of Elevation and Azimuthal Angle, $\lambda = 0.25$ m and $\sigma = 0.2$ m

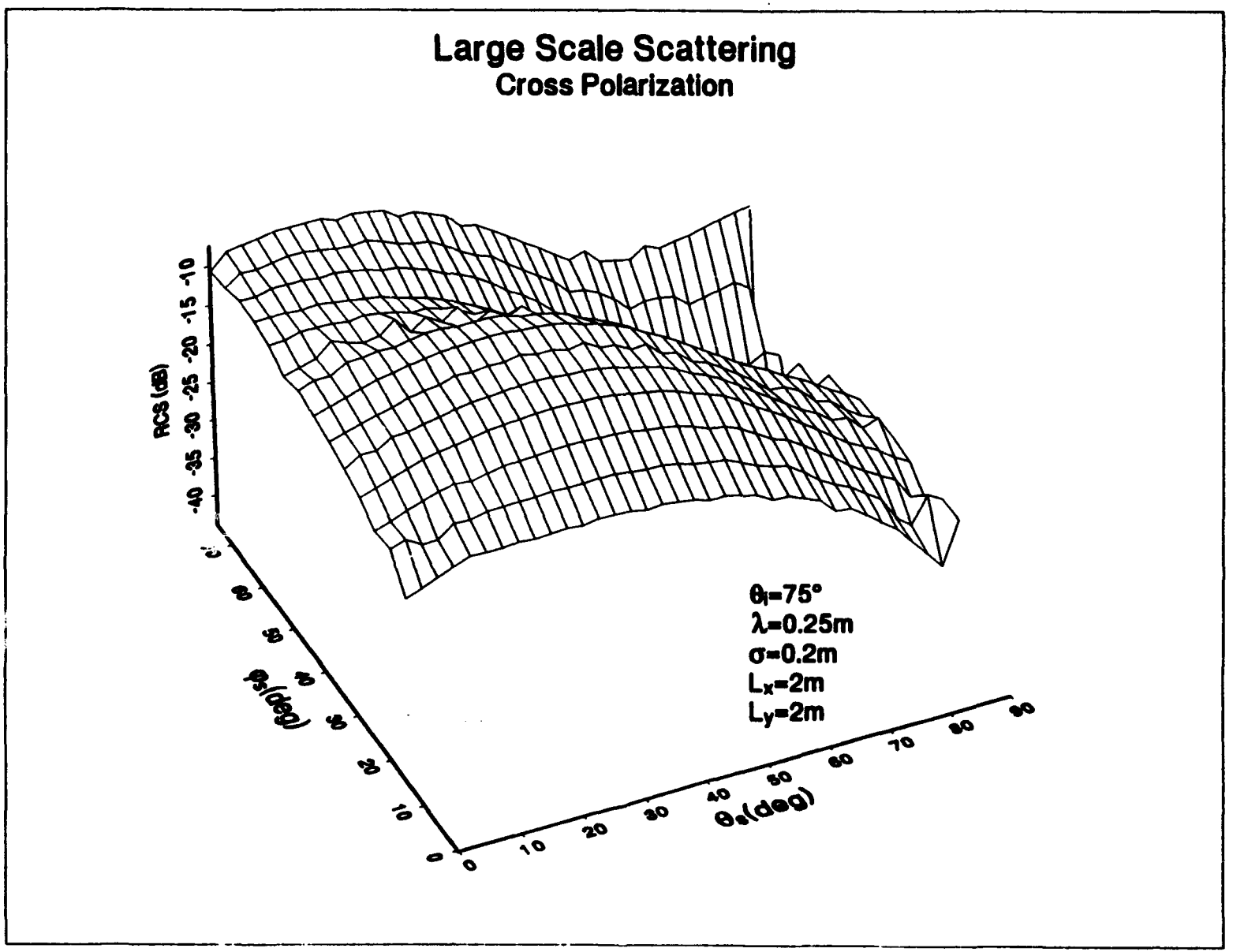


Figure 6. Cross-Polarized Normalized Scattering Cross Section as a Function of Elevation and Azimuthal Angle, $\lambda = 0.25$ m and $\sigma = 0.2$ m

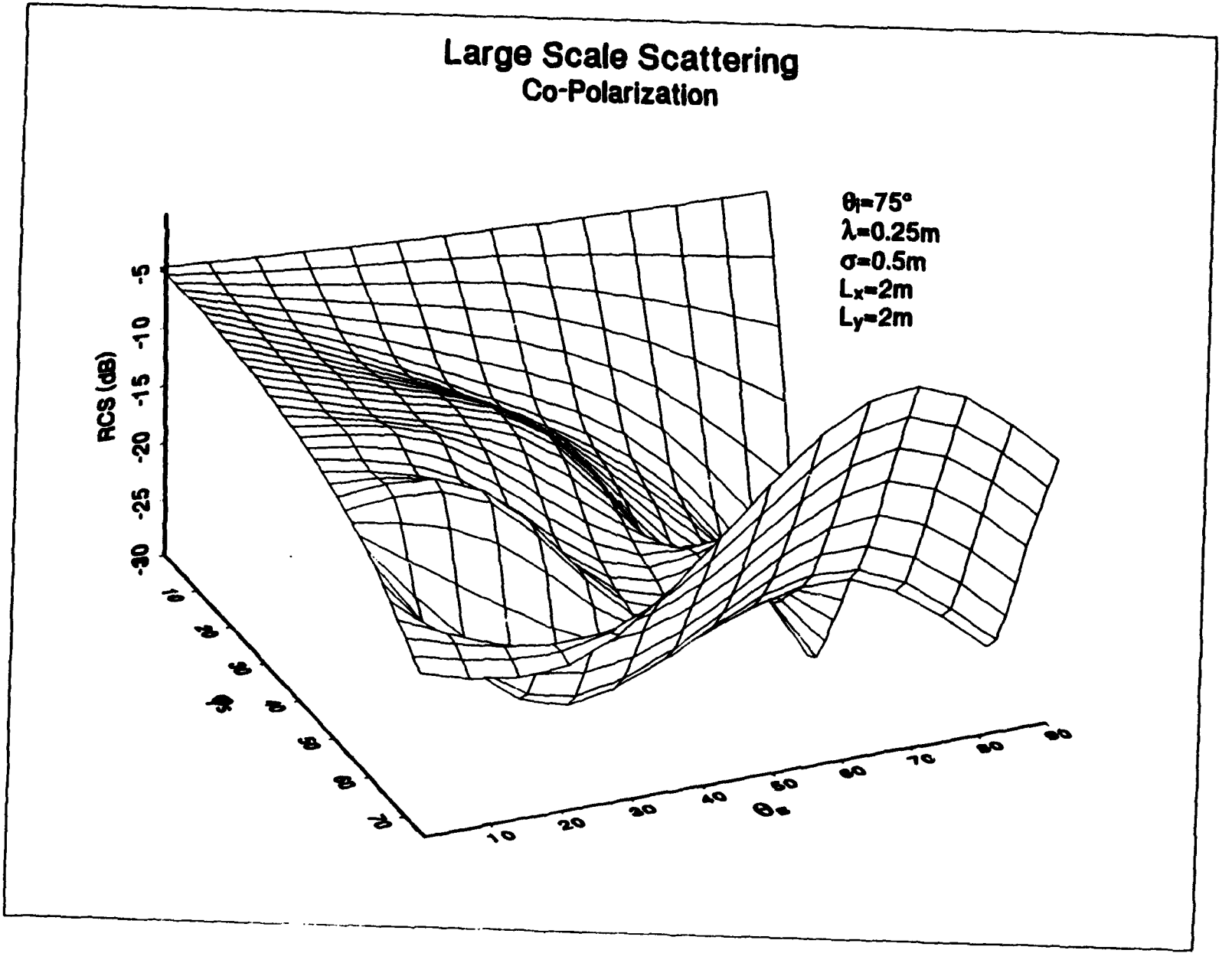


Figure 7. *Co-Polarized Normalized Scattering Cross Section as a Function of Elevation and Azimuthal Angle,* $\lambda = 0.25$ m and $\sigma^* = 0.5$ m

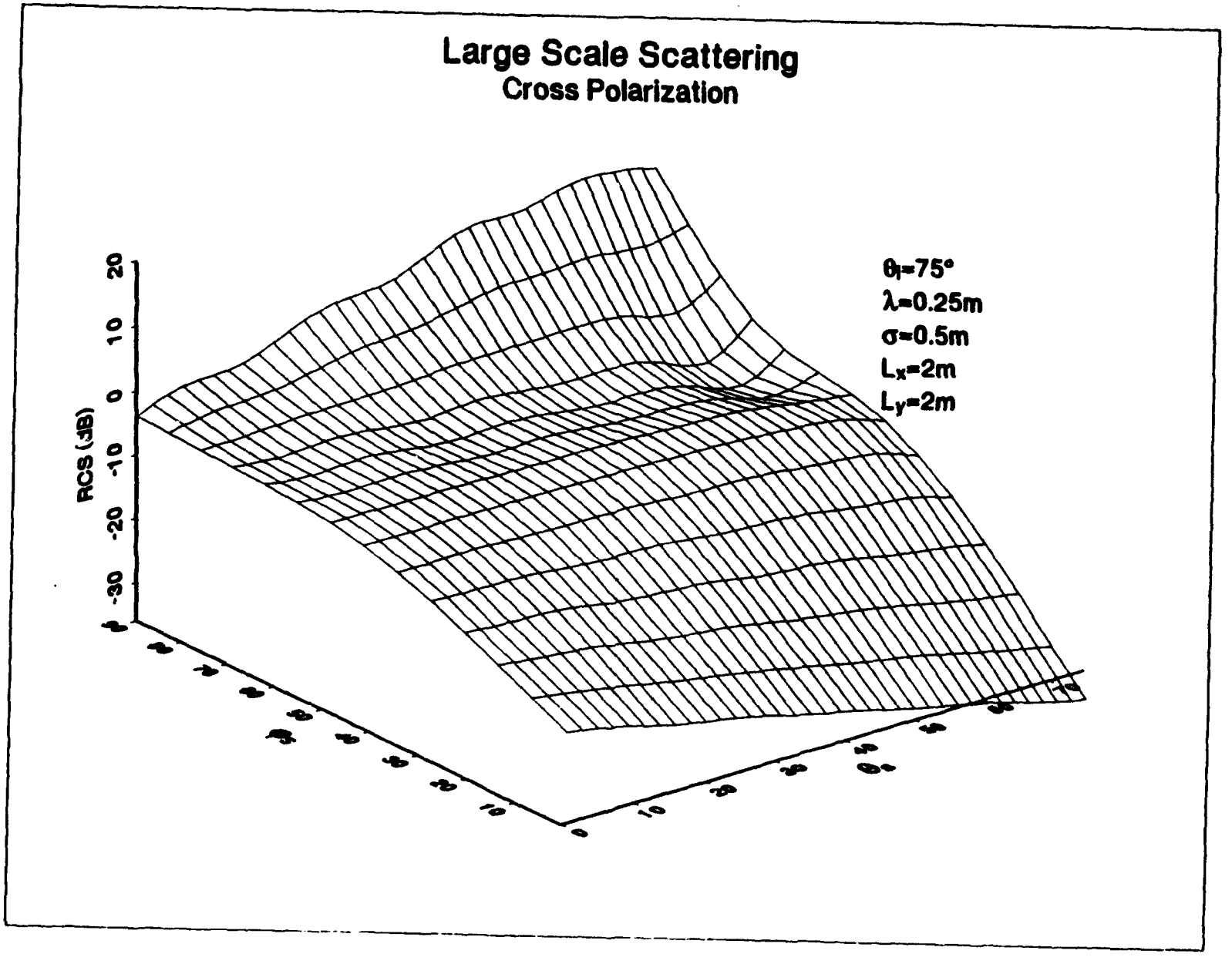


Figure 8. Cross-Polarized Normalized Scattering Cross Section as a Function of Elevation and Azimuthal Angle, $\lambda = 0.25$ m and $\sigma = 0.5$ m

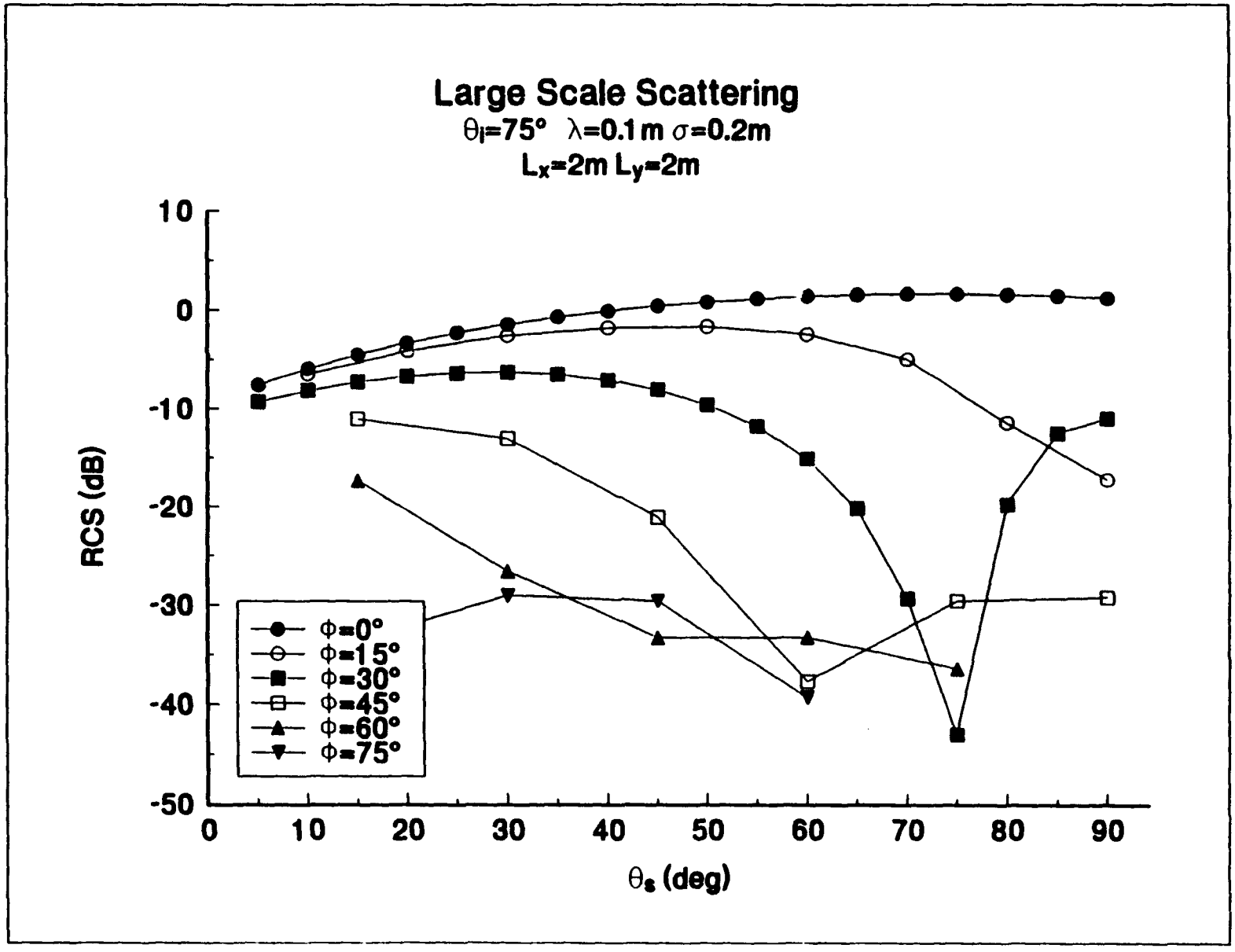


Figure 9. Co-Polarized Normalized Scattering Cross Section as a Function of Elevation Scattering Angle for Selected Azimuthal Angles, $\lambda = 0.1$ m and $\sigma = 0.5$ m

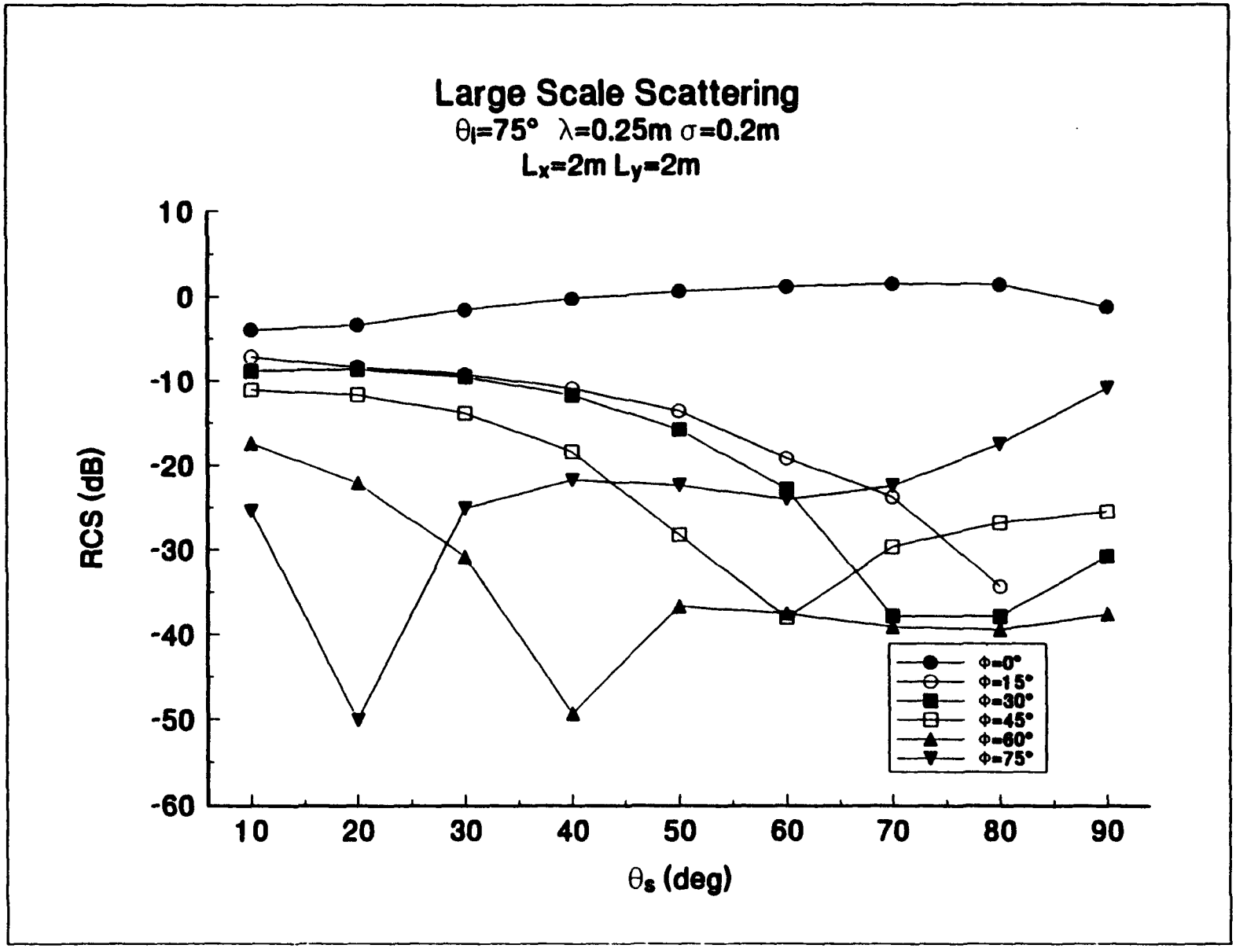


Figure 10. Co-Polarized Normalized Scattering Cross Section as a Function of Elevation Scattering Angle for Selected Azimuthal Angles, $\lambda = 0.25$ m and $\sigma = 0.2$ m

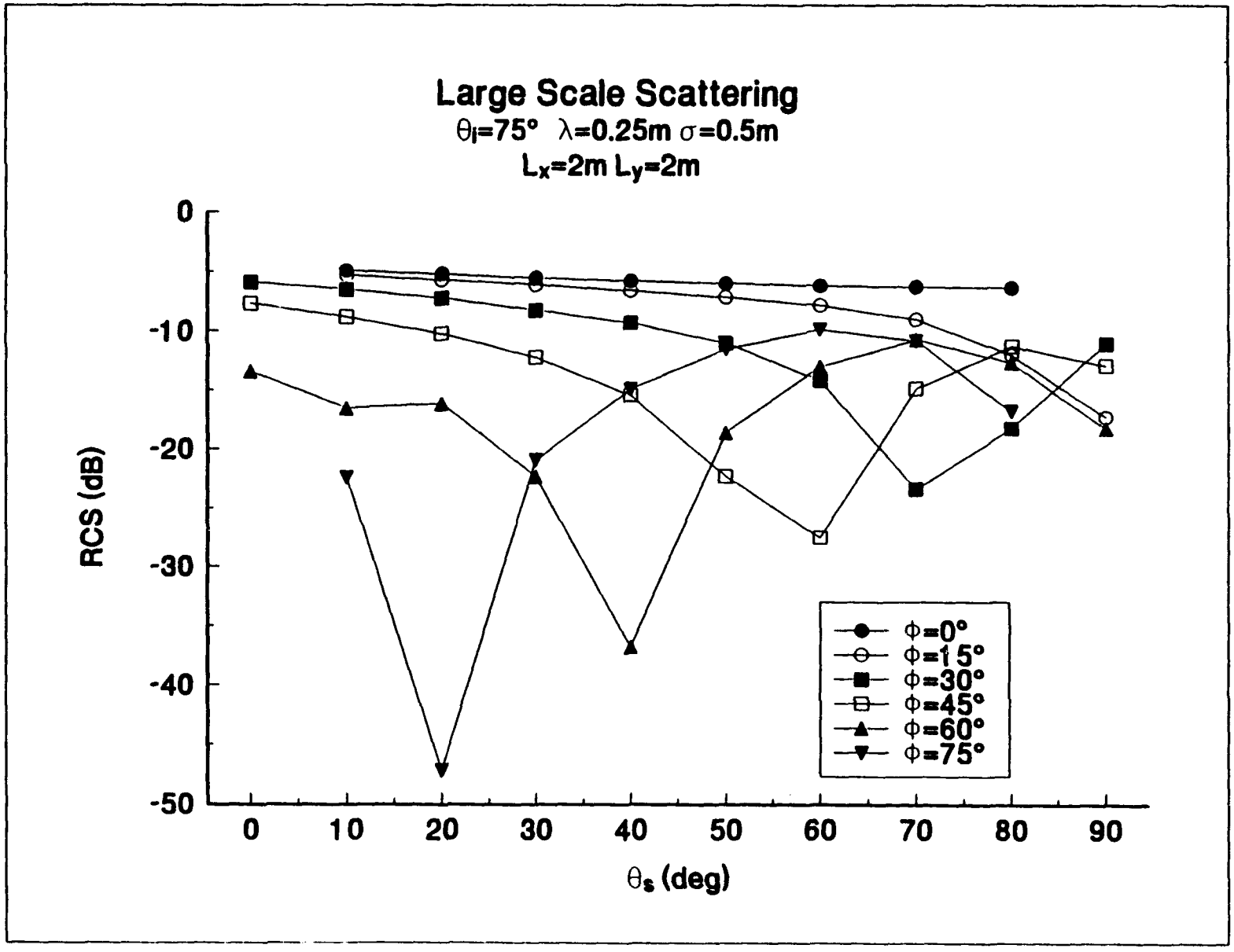


Figure 11. Co-Polarized Normalized Scattering Cross Section as a Function of Elevation Scattering Angle for Selected Azimuthal Angles, $\lambda = 0.25$ m and $\sigma = 0.5$ m

## 4. CONCLUSIONS

This report describes the extension of the analysis of finite cell size effects to the more significant case of bistatic scattering at arbitrary angles from a surface with roughness that varies in two dimensions. This introduces more complexity into the analysis than for the earlier one-dimensional studies both from the range of angular conditions to be considered and the fact that the effects of scattered signal depolarization must be included. In this report we have described a number of trends that can be seen in the results.

Previous results for determining clutter power have used a physical optics model that assumes the cell size is very large relative to the correlation distance. To determine the effect of reducing the cell size on the clutter power, the results for the finite cell size and infinite cell size were compared. The polarization nulls were found to be unaffected by the size of the clutter cell. This result is not surprising, however, because the null location is in general a function of the scattering configuration. The magnitude of $\sigma^o$, however, does depend on the integration limits and hence is affected by cell size. The normalized clutter power from the smaller cell is consistently less than for the infinite cell size, particularly in the near forward scatter direction. The results confirmed that the null locations in the overall patterns are insensitive to wavelength or roughness variations. The depolarization of the scattered wave shows that in the regions where the co-polarized component decreases, the cross polarized component increases.

The next aspect of interest is comparisons with other calculations. The results obtained by the model given in this report for a two-dimensionally rough surface were compared to results given by the simpler one-dimensionally rough surface model in the limit as $L_y \to 0$. The agreement between the two models was quite good except for extreme forward and extreme backscatter directions. The question of how the finite cell results matched those for the infinitely large case also showed that the patterns for increasing cell size rapidly approached the large cell results.

A related result seen is that increasing the cross range dimension of the clutter cell has very little effect on $\sigma^o$. This is a significant result because in high resolution radars, it is the range dimension that decreases, while the cross range dimension can remain quite large. It should be pointed out that the integral for $\sigma^o$ does depend on which limits are varied.

Finally, it should be pointed out that the subject of two-dimensional finite cell scattering is a highly complex topic. This initial study has related the behavior of the scattering to a number of different sets of results and has shown important findings for high resolution radars. Future studies still have to address additional aspects. The normalized clutter cross section of a clutter cell with finite dimensions can be calculated by numerically solving a double integral. The variance of the clutter power, however, requires the solution of an eight-fold integral that is numerically intensive and quite complicated. This will be pursued in subsequent efforts.

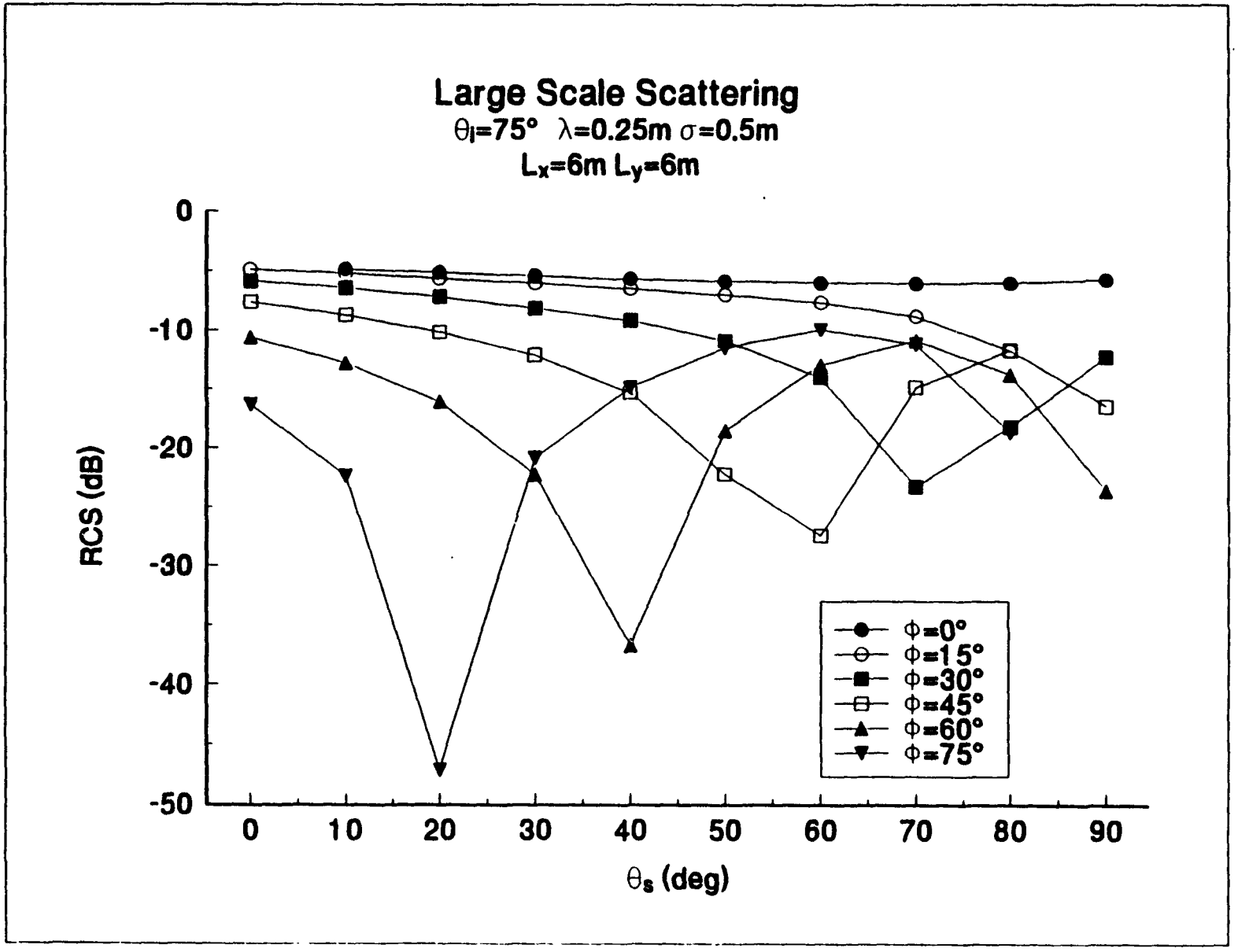


Figure 12. Co-Polarized Normalized Scattering Cross Section Behavior for Increased Cell Size, Lx = Ly = 6 m

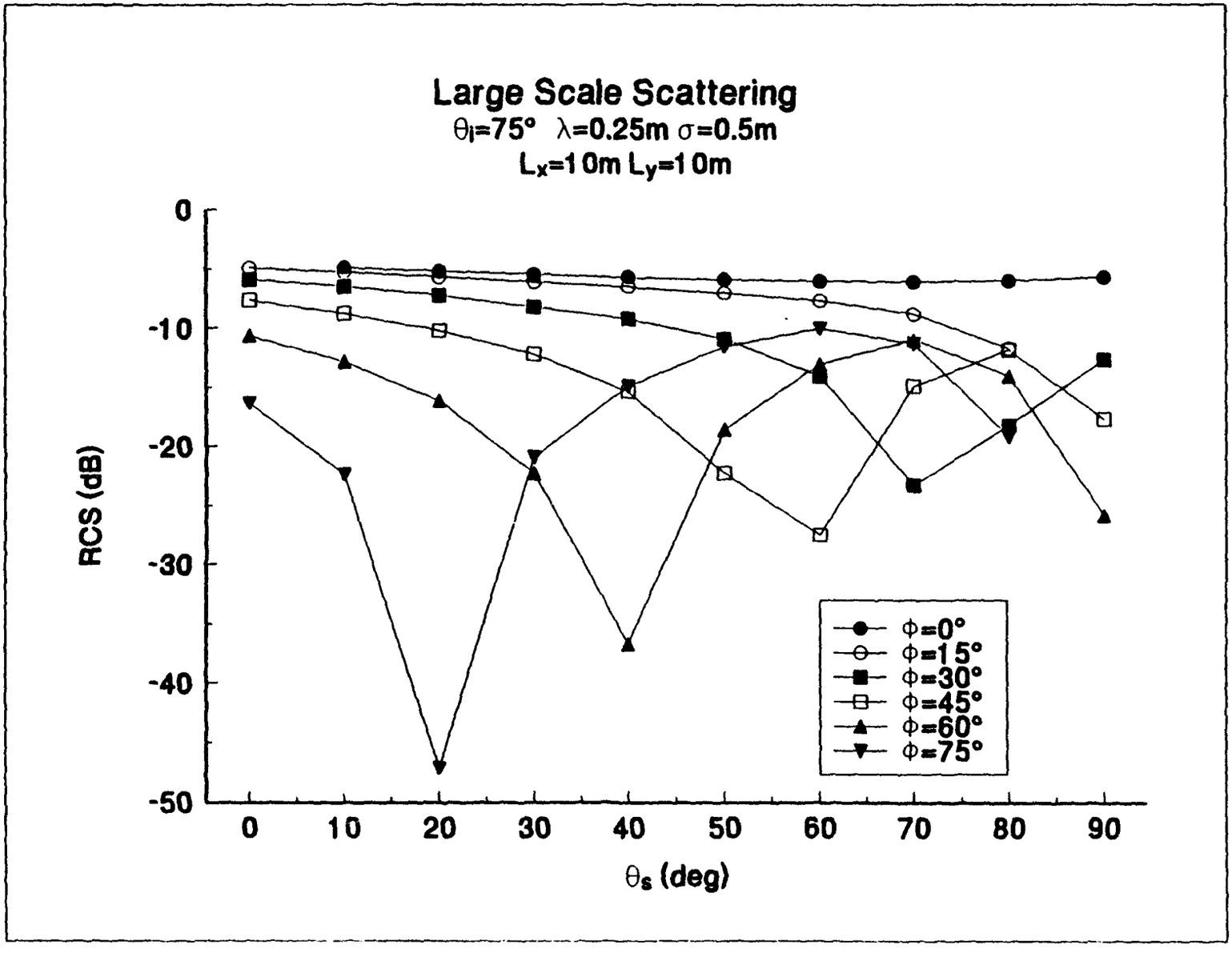


Figure 13. Co-Polarized Normalized Scattering Cross Section Behavior for Increased Cell Size, Lx = Ly = 10 m

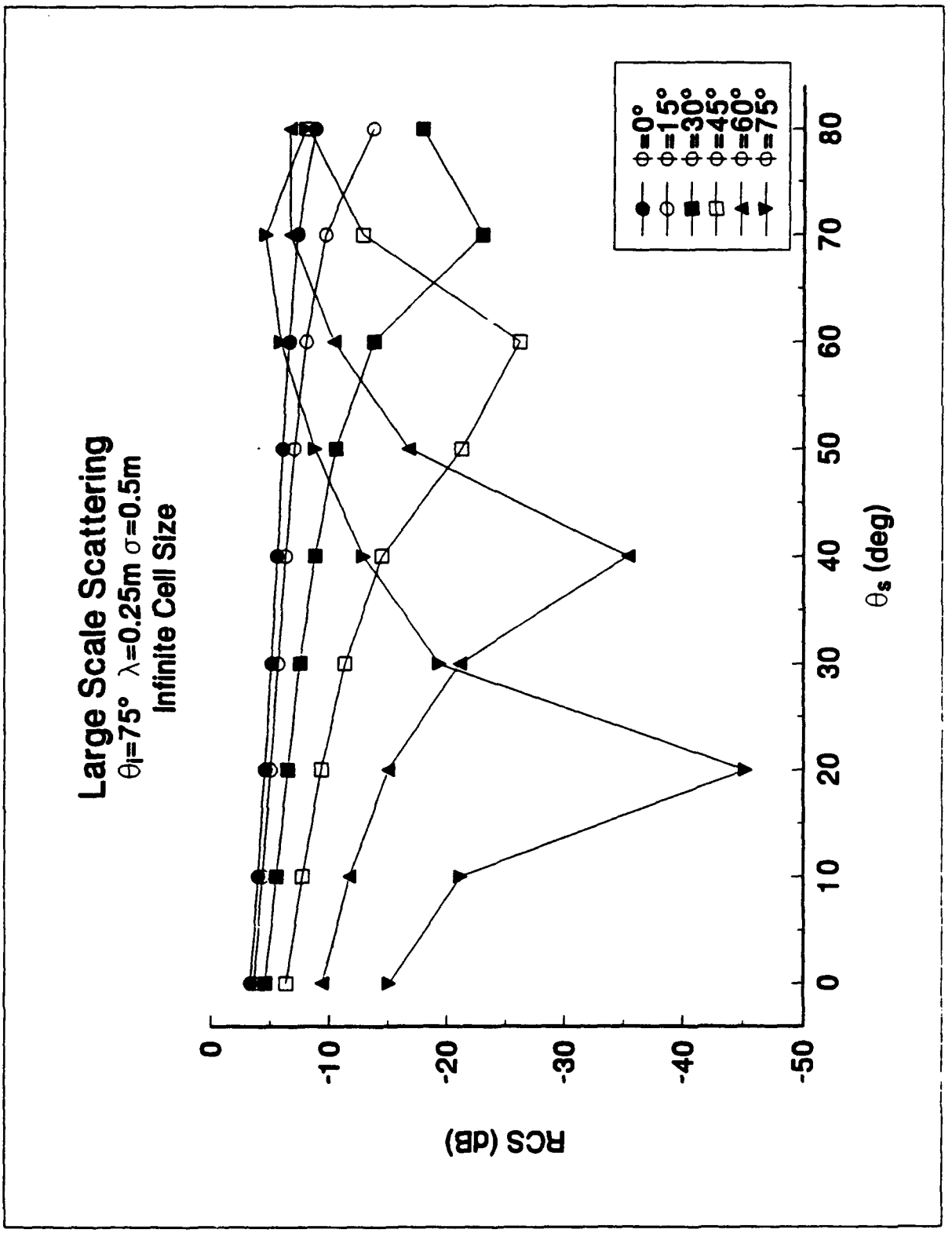


Figure 14. Co-Polarized Normalized Scattering Cross Section Behavior for Increased Cell Size, Infinite Cell Area Result

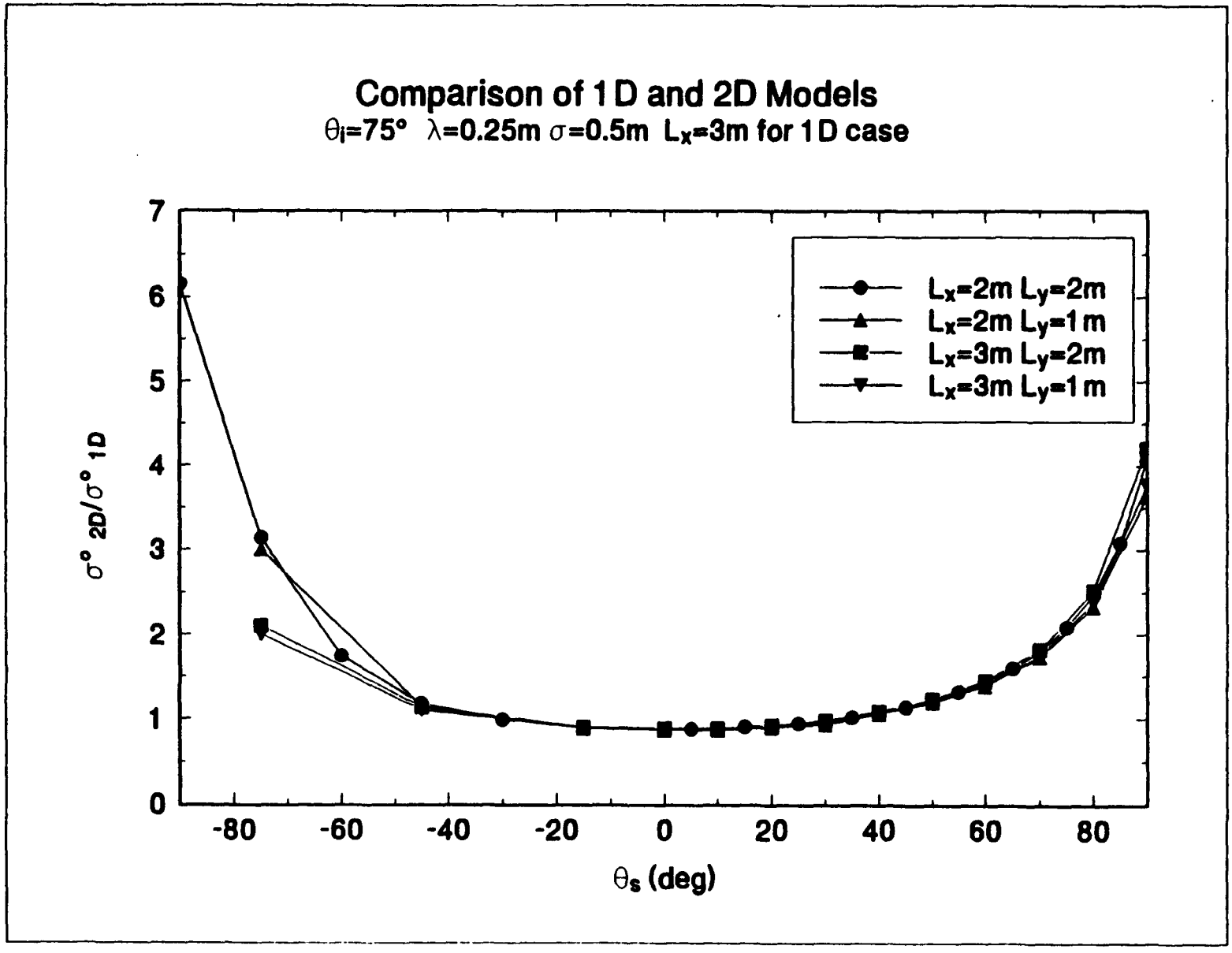


Figure 15. Comparison of Cross Section Results for One-Dimensional Model with Those for Successively Smaller Two-Dimensional Cells

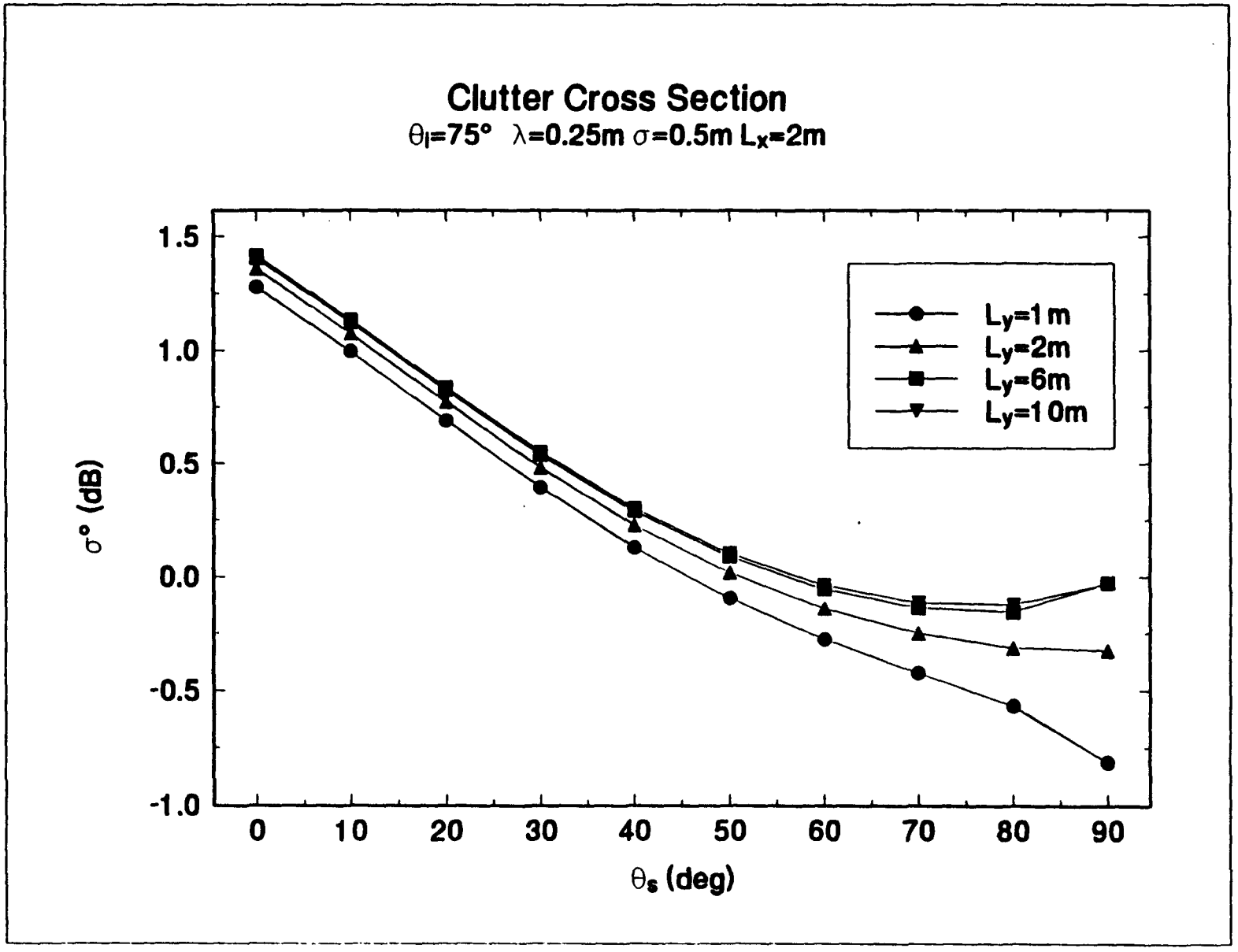


Figure 16. Normalized Scattering Cross Section Results for Cells with Increasing Azimuthal Extents, In-Plane Scattering

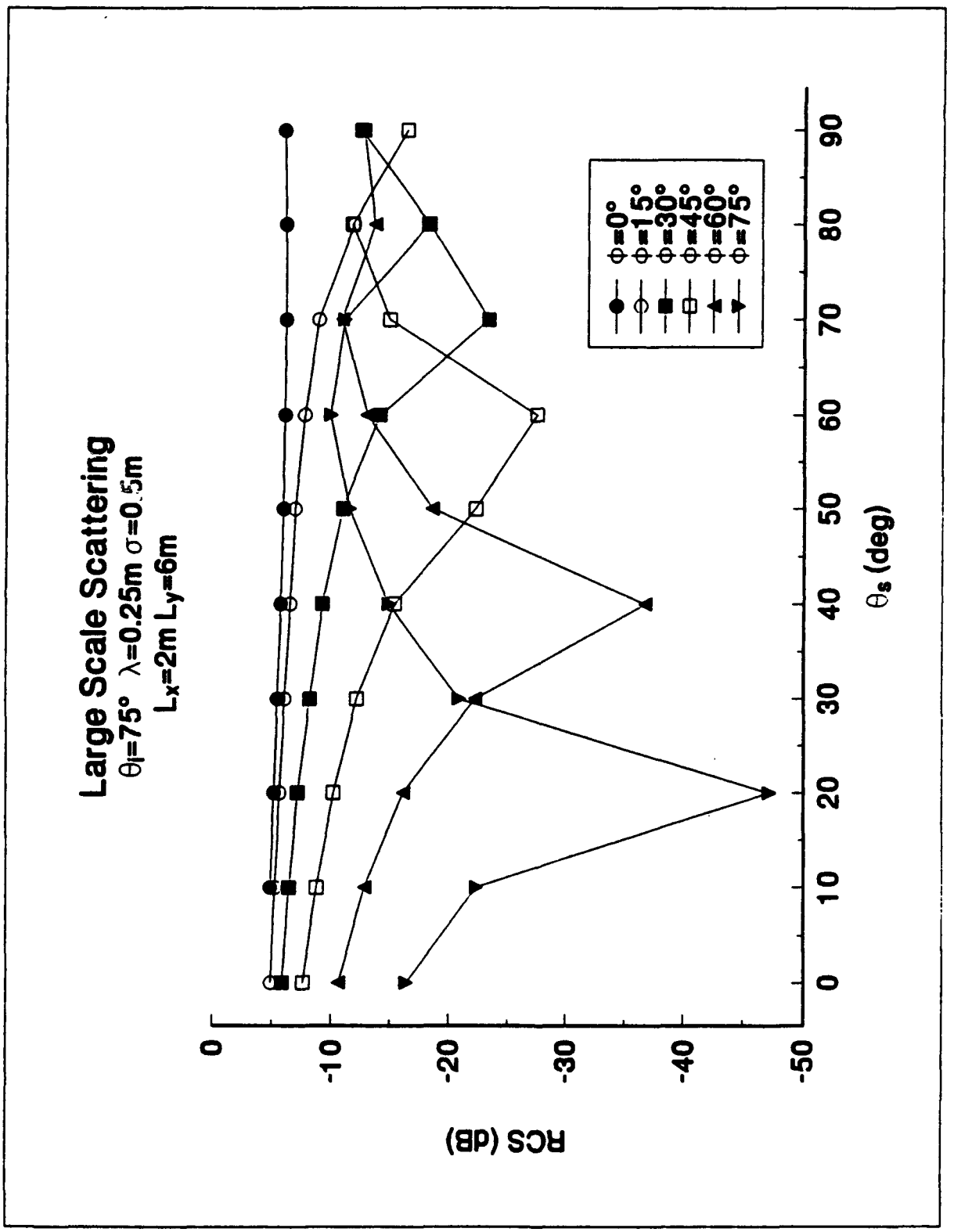


Figure 17. Normalized Scattering Cross Section Results at Selected Azimuthal Angles for Lx = 2 m and Ly = 6 m

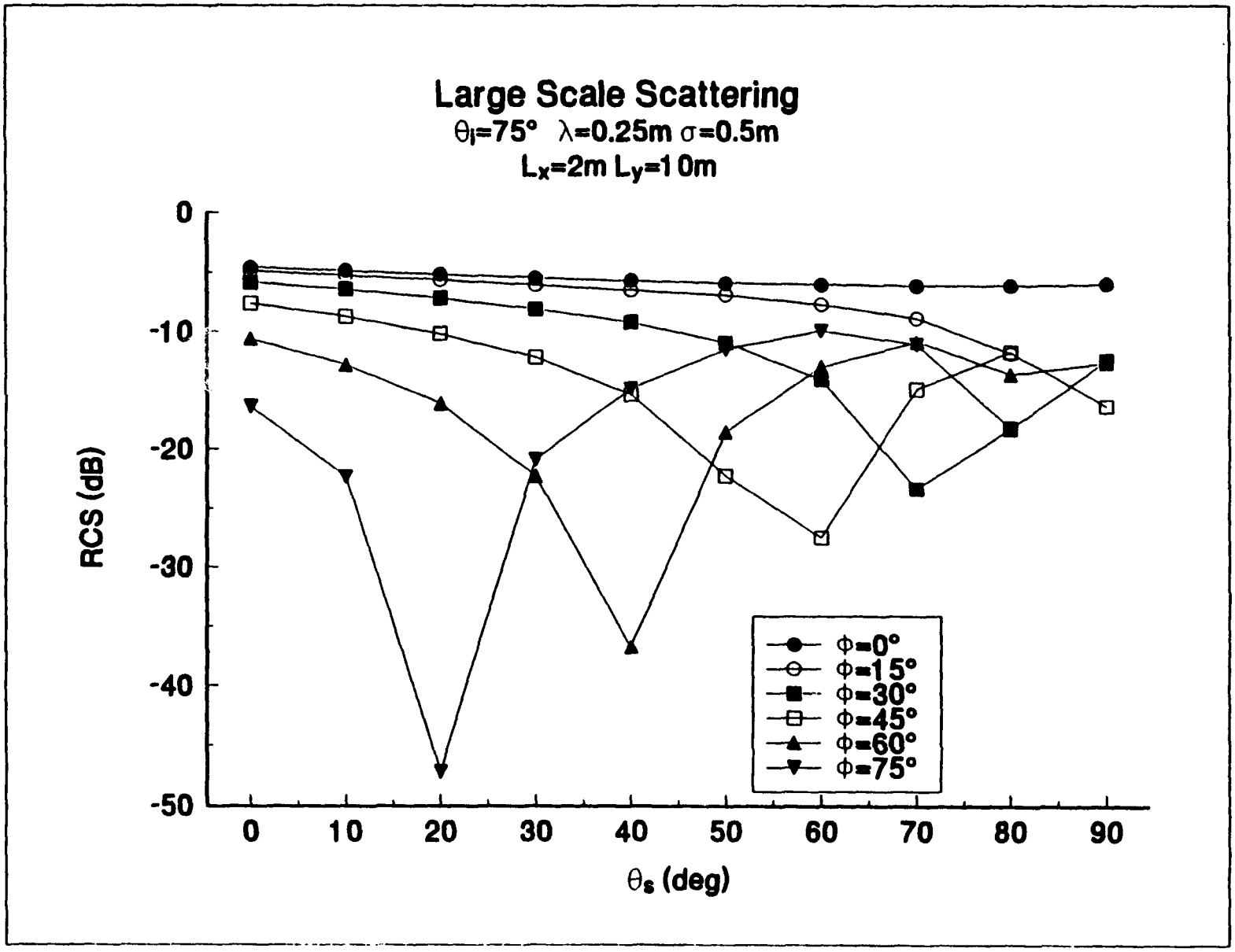


Figure 18. Normalized Scattering Cross Section Results at Selected Azimuthal Angles for Lx = 2 m and Ly = 10 m

## References


1. Papa, R.J., and Woodworth, M.B. (1991) *The Mean and Variance of Diffuse Scattered Power as a Function of Clutter Resolution Cell Size*, RADC-TR-91-09. **ADA253897**

2. Sharpe, L.M. (1991) *Analytical Characterization of Bistatic Scattering from Gaussian Distributed Surfaces*, RL-TR-91-351. **ADA254253**

3. Sharpe, L.M. (1992) Analytical Characterization of Bistatic Scattering from Rough Surfaces: Dependence on Surface Correlation Function, RL-TR-92-134. **ADA256525**

4. Papa, R.J., Lennon, J.F., and Taylor, R.L. (1986) The Variation of Bistatic Rough Surface Scattering Cross Section for a Physical Optics Model, *IEEE Trans. Antennas and Propagation*, **AP-34** (No. 10).

## *MISSION*

## *OF*

## *ROME LABORATORY*

*Rome Laboratory plans and executes an interdisciplinary program in research, development, test, and technology transition in support of Air Force Command, Control, Communications and Intelligence ($C^3I$) activities for all Air Force platforms. It also executes selected acquisition programs in several areas of expertise. Technical and engineering support within areas of competence is provided to ESD Program Offices (POs) and other ESD elements to perform effective acquisition of $C^3I$ systems. In addition, Rome Laboratory's technology supports other AFSC Product Divisions, the Air Force user community, and other DOD and non-DOD agencies. Rome Laboratory maintains technical competence and research programs in areas including, but not limited to, communications, command and control, battle management, intelligence information processing, computational sciences and software producibility, wide area surveillance/sensors, signal processing, solid state sciences, photonics, electromagnetic technology, superconductivity, and electronic reliability/maintainability and testability.*